PNAS

Double stress of waterlogging and drought drives forest–savanna coexistence

Caio R. C. Mattos[a,1] (ID), Marina Hirota[b,c,d] (ID), Rafael S. Oliveira[c] (ID), Bernardo M. Flores[d], Gonzalo Miguez-Macho[e], Yadu Pokhrel[f] (ID), and Ying Fan[a] (ID)

Forest–savanna boundaries are ecotones that support complex ecosystem functions and are sensitive to biotic/abiotic perturbations. What drives their distribution today and how it may shift in the future are open questions. Feedbacks among climate, fire, herbivory, and land use are known drivers. Here, we show that alternating seasonal drought and waterlogging stress favors the dominance of savanna-like ecosystems over forests. We track the seasonal water-table depth as an indicator of water stress when too deep and oxygen stress when too shallow and map forest/savanna occurrence within this double-stress space in the neotropics. We find that under a given annual precipitation, savannas are favored in landscape positions experiencing double stress, which is more common as the dry season strengthens (climate driver) but only found in waterlogged lowlands (terrain driver). We further show that hydrological changes at the end of the century may expose some flooded forests to savanna expansion, affecting biodiversity and soil carbon storage. Our results highlight the importance of land hydrology in understanding/predicting forest–savanna transitions in a changing world.

forest savanna transitions | Amazon | hydrology | tropical ecology

The distribution of forests and savannas in the Neotropics has long been linked to large-scale rainfall patterns (Fig. 1*A*). Forests dominate where rainfall is high, whereas savannas dominate where it is low, with a range of rainfall conditions in between where both vegetation types coexist (1, 2). One theory explaining this coexistence considers forests and savannas as alternative stable states (*SI Appendix,* Fig. S1 *B* and *C*); i.e., both are possible states, but shifting from one to the other through disturbances in mean annual precipitation (MAP), fire, herbivory, and consequent feedbacks (1–4). This theory is consistent with the fact that forest–savanna boundaries are often narrow in space because positive feedbacks tend to stabilize the vegetation in one of the stable states (3).

At the landscape scale, topography redistributes water from hills to valleys and determines how quickly excess water can be drained, creating fine-scale mosaics of excessive, adequate, and poorly drained patches (or niches) under the same rainfall (*SI Appendix,* Fig. S2). While under the hills the water table (WT) is deep, and plants rely mostly on past rainfall stored in the soil, a shallow WT in the valleys can provide plants with sufficient water to meet dry-season evapotranspiration demand (5). However, when the WT is too shallow, fluctuating within the root zone, the stress of waterlogging and anoxia stresses plants and limits rooting depth (6, 7). The "hydrologic niche theory" argues that species segregate according to trade-offs from drought adaptations in one end to waterlogging adaptations in the other (8–10). In between lies the physiological challenge of tolerating double stresses alternating between the wet (waterlogging) and the dry (drought) seasons.

Empirical evidence and ecological theory suggest an inherent conflict or trade-off between plant traits adapting to waterlogging and those adapting to drought (11, 12). Waterlogging restricts roots to shallow depths, while deeper roots are often needed to escape drought, and seasonal switching between shallow and deep roots would require fast root turnover, imposing high metabolic costs at the expense of biomass production (13), thus favoring species that can complete full aboveground life cycles in a short season, replacing aerial organs following the waterlogging and drought cycles (14). This framework of vegetation tolerance to multiple abiotic stresses (11) has been useful for understanding species distribution at the local level based on their ability to cope with these stresses (8–10, 15). However, the tradeoff in the context of double stresses, central to the niche hypothesis, has mostly been demonstrated for herbaceous species, in the strict sense of ref. 8. Here, we test this hypothesis at the ecosystem level to explain forest–savanna coexistence across tropical South America.

Here, we suggest that in lower topographic positions subject to high variability in the WT—too deep in the dry season and too shallow in the wet season—vegetation faces the "double stress" of waterlogging and drought. We hypothesize that the intensity of the

Significance

Explaining the distribution of vegetation is a long-standing challenge in ecology. In the tropics, forests have been associated with areas of high rainfall and low fire occurrence, while savannas dominate where rainfall is lower, and fire is frequent. However, in many landscapes, both vegetation types coexist, with savanna (forest) pockets occurring within forest (savanna) dominated areas. Using modeling and remote sensing, we show that one mechanism driving this coexistence is hydrology. In areas where the water table varies seasonally from too shallow (waterlogging) to too deep (drought), savannas are favored even if rainfall is high. Considering this mechanism alters our predictions of forest–savanna dynamics under a changing climate.

double stress combined with rainfall seasonality filters out high tree cover vegetation (forest) and favors low tree cover, savanna-like vegetation. To test our hypothesis, we use remotely sensed tree cover as a first-order indicator of vegetation structure, excluding all pixels affected by anthropogenic land use change (*SI Appendix*), and following the conventional tree cover threshold of 60% to distinguish between forests (above 60%) and savannas (below), as

in previous studies of the tropics (1). While we fully appreciate the wide-ranging life histories, functional types, species, and ecological strategies arising from the immense biodiversity of forest–savanna transitions, here we use a simple threshold, based on the multimodal distribution of tropical vegetation (1, 2), differentiating between forests and savannas to focus on the basic hydrologic mechanisms which shape the first-order vegetation structure.
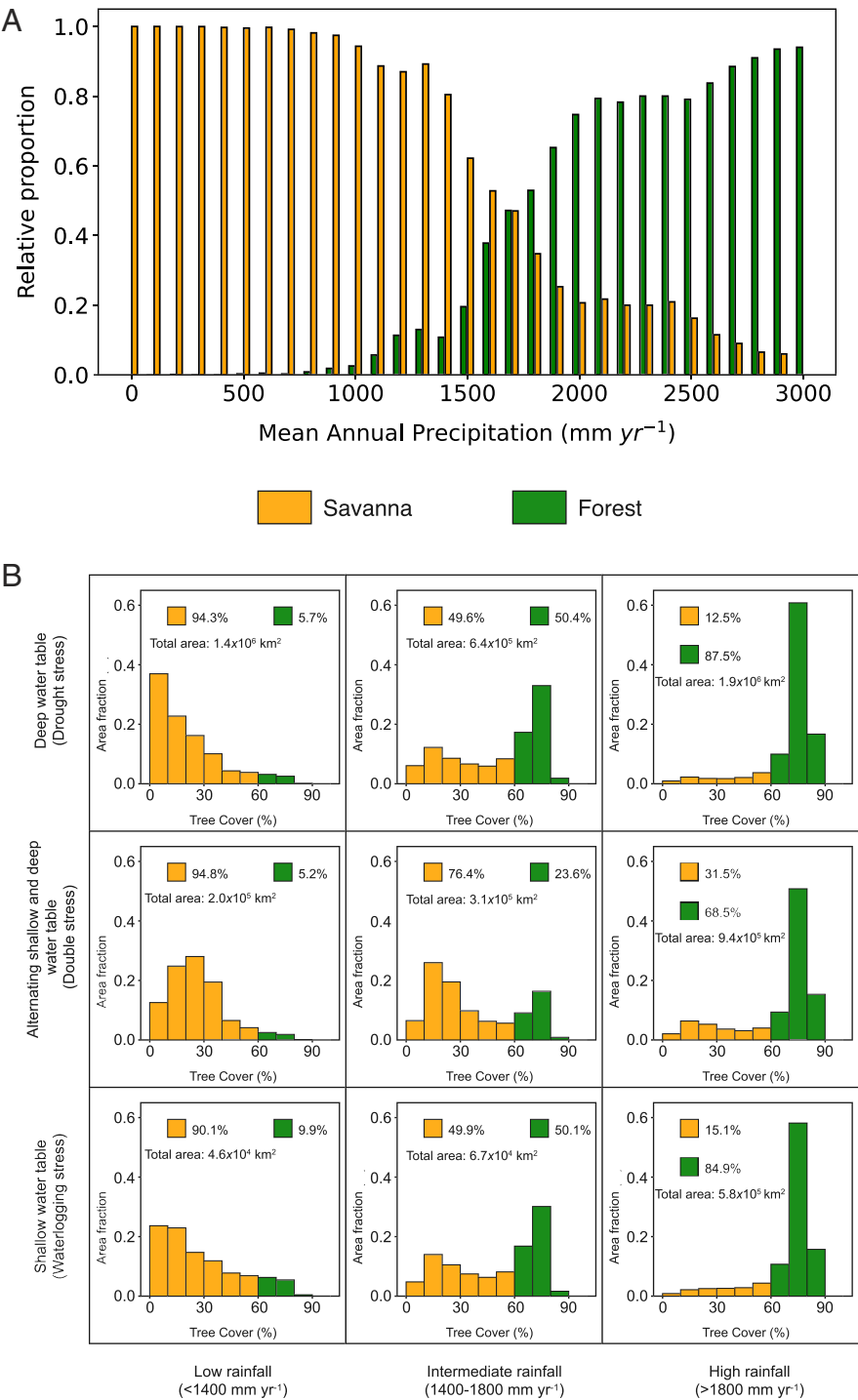

Fig. 1. Rainfall and water table variability control patterns of forest–savanna abundance across tropical South America. (*A*) Forest (tree cover > 60%) and savanna occurrence along annual rainfall gradient. We define three rainfall classes based on potential analysis (*SI Appendix*, Fig. S1): low (<1,400 mm y^{-1}, where only savannas are stable), intermediate (1,400 to 1,800 mm y^{-1}, where forests and savannas are bistable), and high (>1,800 mm y^{-1}, where forests are stable). We use three drainage classes based on sum exceedance values: deep water table (drought stress, water table always below 2 m); alternating shallow and deep water table (WT fluctuates above 0.25 m and below 2 m); and shallow water table (always shallower than 0.25 m). (*B*) Histograms showing tree cover distribution in each rainfall-drainage class, with relative abundance of forest and savanna. Increasing rainfall systematically favors higher tree cover vegetation, while along drainage gradient, forest cover is the lowest at the fluctuating WT class, at which landscape positions vegetation experiences double stress.

We use monthly WT depth as a first-order indicator of drought (WT too deep too often) and waterlogging (WT too shallow too often), following the seminal study of Silvertown et al. (8). However, very few WT observations exist (*SI Appendix*, section 4.3) that i) can resolve seasonal dynamics for more than one growing season; ii) sampled the full range of land drainage conditions from excessively drained plateaus to perennial waterlogged floodplains; and iii) span the full range of seasonality in rainfall across the neotropics. Thus, we resort to a continental high-resolution (~1 km) inverse hydrologic model, that uses the observed climate, leaf area index, soil, and topography to constrain the resulting seasonal WT dynamics, at daily steps over 15 y (2004 to 2018) (5). We validated our model results against available observations at 103 flux-towers, 4,885 groundwater wells for annual mean and 12 wells for seasonal WT depth, 34 river basin stream gages, and GRACE-satellite terrestrial water storage change at 6 representative windows in Amazônia (5° × 5°) (see *Materials and Methods* and *SI Appendix*, section 3 for details). Without any calibration, our model reproduces the observed seasonal dynamics of evapotranspiration (point-scale vertical flux, soil to atmosphere), WT depth (point-scale storage via vertical recharge and lateral hill-to-valley convergence), drainage basin water balance (areal integrated 2-way groundwater-river exchange modulated by channels-floodplains), and terrestrial water storage (vertical integrated soil, surface, and groundwaters over large domains), thus constraining hydrologic stores and fluxes in three dimensions at point to Amazon basin scales. We consider our model results sufficiently realistic for assessing the impact of seasonal land hydrology on first-order vegetation structures. We fully acknowledge that models are not observations, but in the absence of observations, mechanistic models that capture the basic hydrologic processes and are validated with available observations at multiple scales allow us to achieve our goals.

We note that the model simulated WT dynamics reflect vegetation water uptake determined from satellite-observed seasonal biomass (leaf area index). Transpiration from large biomass during the dry season drives high soil water uptake, which is distributed by Ohm's law to multiple soil layers (6), and the dynamic root uptake driven by satellite-derived biomass effectively lowers groundwater recharge and WT depth. The effect of plant uptake on WT depth can be appreciated by comparing the mean WT without dynamic root uptake (*SI Appendix*, Fig. S3A after ref. 16) vs. with dynamic and deep root uptake (6), the latter including vegetation feedback on the physical hydrology (*SI Appendix*, Fig. S3B).

Drainage and Climate Controls on Tree Cover

To determine the effects of climate on forest–savanna coexistence, we first use potential analysis (*SI Appendix*) using tree cover from the Moderate Resolution Imaging Spectroradiometer (MODIS) satellite and MAP from ERA5 (17) to divide tropical South America into three rainfall classes (Fig. 1*B*, columns): low (<1,400 mm y^{-1}), where savanna is the only stable state; intermediate (between 1,400 and 1,800 mm y^{-1}), where both savannas and forests are possible stable states; and high rainfall (above 1,800 mm y^{-1}), where forests are the only stable state. Then, to explicitly describe the role of land drainage in shaping vegetation distribution at smaller spatial scales than climate, we use our 15-y monthly time series of WT depth to create three drainage classes (Fig. 1*B*, rows): stable, deep WT (always below 2 m); stable, shallow WT (always above 0.25 m); and unstable WT, alternating between too shallow (above 0.25 m) and too deep (below 2 m). For each combination of rainfall-drainage class, we quantify the relative abundance of forest vs. savanna (Fig. 1*B*) by first classifying a pixel as either forest or savanna (using the 60% tree cover threshold

mentioned above) and then computing the area occupied by either vegetation types. This approach allows us to differentiate the structuring effects of i) changing rainfall for the same drainage positions and ii) changing drainage conditions under the same rainfall.

Forest vs. savanna coexistence is modulated by both rainfall and drainage. Independently of drainage position, forest abundance increases as rainfall increases (Fig. 1 *B*, *Left* to *Right*), consistent with increasing water supply and decreasing seasonality, which is highly correlated with rainfall totals in the study area. Feedback mechanisms favoring the forest state also get stronger with increasing rainfall, such as reduced fire frequency and intensity (3, 4). Stable drainage positions, either too deep or too shallow, do not seem to influence the relative proportion of forests and savannas across rainfall classes. They mirror the pattern predicted by rainfall alone, except perhaps for a small increase in forest proportion in low rainfall but shallow WT areas, consistent with groundwater-supplied riparian forests in savannas (18).

Where an unstable WT is present, with alternating waterlogging and drought stresses, savannas are highly favored and show greater proportions than in other drainage positions in all three rainfall classes. This is most striking in the intermediate rainfall class, thus pointing to hydrologic regulation of forest and savanna coexistence in the "bistability range", where both states are stable according to rainfall levels alone. These results show that hydrology provides another axis of environmental control on the abundance of forests and savannas in the bistability range and is thus able to initiate vegetation state shifts if variability (and thus double stress) increases.

We thus expect forests and savannas to occupy unique positions in a hydrological space defined by waterlogging stress and drought stress. Following ref. 8, we define hydrological stress using the sum exceedance values (SEV), which in our case represent the number of months in a year when the WT is above or below a certain threshold for each model cell. For drought stress, we calculate the drought SEV using the number of months the WT is deeper than 2 m. For the waterlogging SEV, we use the number of months the WT is shallower than 0.25 m. We then use a 2-dimensional space to evaluate forest/savanna abundance in each combination of drought and waterlogging stress.

We first build a conceptual model, where flooded forests occupy the leftmost column of zero drought stress but varying degrees of waterlogging. Terra firme forests and upland savannas occupy the lowermost row of zero waterlogging but varying degrees of drought stress. From the lower left corner moving up diagonally, the frequency of double stress increases, forest abundance progressively decreases, and savannas become the dominant vegetation type along the "boundary line" (as defined by ref. 12) of the hydrological stress space where double stress is the highest. We then show in Fig. 2*B* our results, using the SEVs derived from modeled WT and quantifying the area occupied by forests in all cells belonging to each waterlogging and drought SEV combination, using MODIS Tree Cover.

Savannas increase in dominance as the degree of double stress increases (Fig. 2*B*), in line with our conceptual model. While forests seem progressively favored as the degree of waterlogging stress only increases (leftmost column), and forests and savanna proportions are roughly similar when the only stress is drought (bottom row), savannas become progressively more prevalent as double stress increases (moving diagonally from the origin). This is consistent with our hypothesis and the trade-off postulated by ref. 12, reinforcing that drought and waterlogging combined pose a conflict for vegetation, especially forests (high tree cover), which are replaced by lower tree cover, savanna-like vegetation as double stress increases.
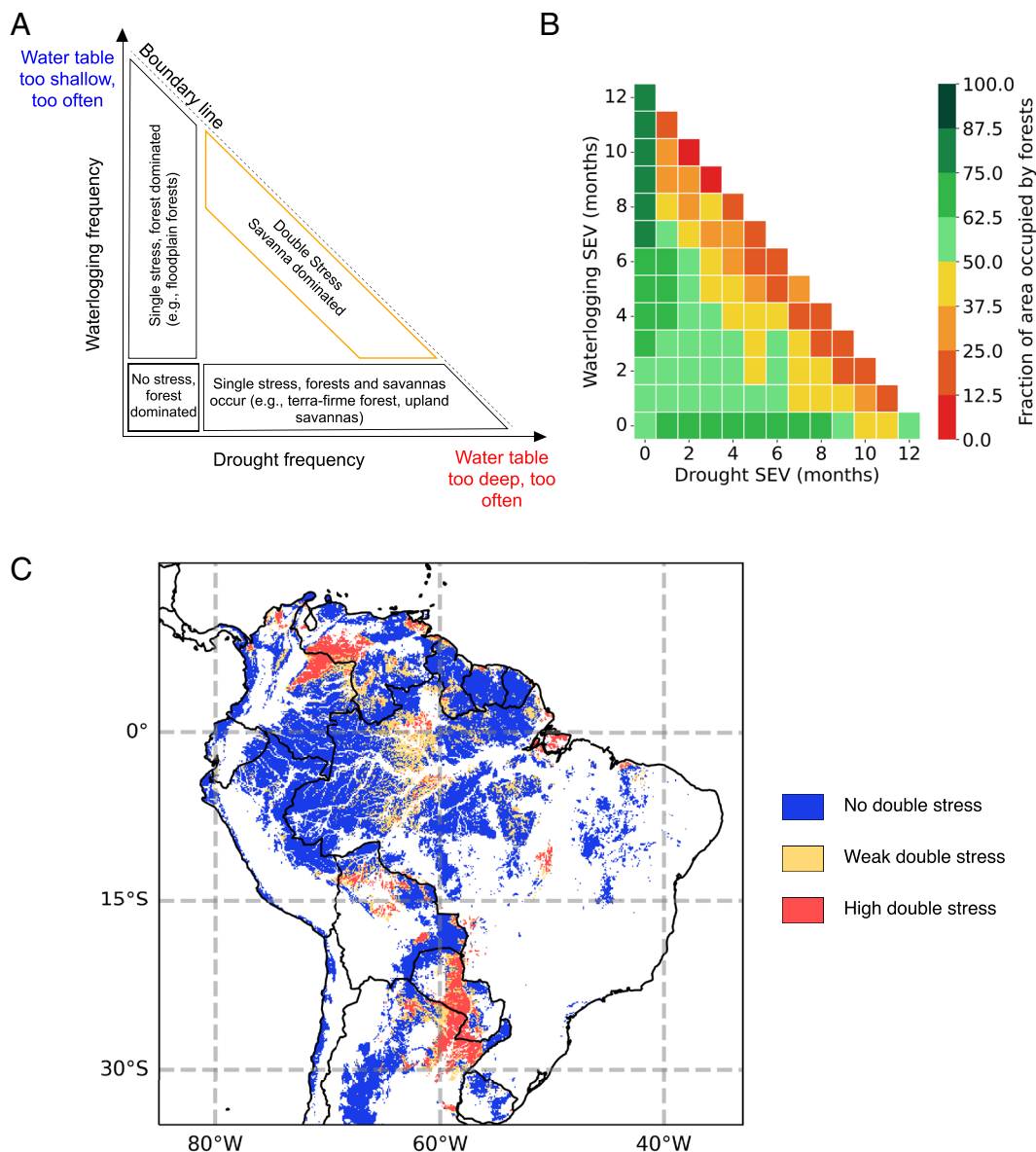
Fig. 2. Double stress of drought and waterlogging jointly define the hydrologic niches for neotropical forests and savannas. (*A*) A conceptual model and hypothesis of likely vegetation structure in the double-stress space. Where vegetation does not suffer from any stress and can continuously access the WT, we hypothesize that forests dominate. In places exposed to drought-only (single stress), forests and savannas are possible states, controlled by factors such as rainfall and seasonality (1, 2). Where waterlogging is the only stress, forests can dominate, especially those with adaptations to prolonged waterlogging such as the floodplain várzea and igapó forests of Amazônia (19). Where double stress occurs, savannas are hypothesized to be the dominant vegetation type. (*B*) Forest dominance (percent of area of forest) in the double stress space, ranging from 0 (savanna-dominated) to 100 (forest-dominated). The horizontal axis shows the frequency in months of WT falling below 2 m depth (drought stress), and the vertical the frequency of WT rising above 0.25 m depth (waterlogging stress); (*C*) a map of South America at the 9 arc-min resolution (~18 km around the Equator) depicting three classes of double stress, defined using the double stress index (DSI): no double stress (single and no stress areas in the conceptual model), weak double stress (e.g., 2 mo of waterlogging, 2 mo of drought, and 8 mo of no stress), and strong double stress (e.g., 6 mo of waterlogging and 6 mo of drought). White pixels correspond to areas excluded from analyses (e.g., open water, agriculture, and high elevations).

We then use the harmonic mean of waterlogging and drought stress to create the double stress index (*SI Appendix*), which we use to classify all cells in our study area according to the degree of double stress (Fig. 2*C*). While weak double stress (few months of alternated drought and waterlogging) can occur in low seasonality areas, such as the floodplains of Central Amazônia, areas exposed to high double stress (closer to 6 mo of drought followed by 6 mo of waterlogging) are mainly on the northern and southern margins of Amazônia where seasonality is higher. Increasing seasonality causes increasing seasonal swings in WT, in and out of plant root zones in a more extreme fashion as the dry season lengthens.

Combining this map and the knowledge of "iconic", long-studied floodplains in tropical South America, we select six locations across a rainfall gradient to explore the effects of double stress at the local-to-regional scale. For each location, we plot i) the distribution of mean monthly rainfall and WT depth to quantify the rainfall and hydrologic stresses and ii) the tree cover distribution for double-stressed areas (dashed line) and non-double-stressed areas (solid line) (Fig. 3).

Double stress, MAP, and seasonality act together to shape the relative distribution of forest and savanna (Fig. 3 and *SI Appendix*, Tables S8 and S9). In the Pastaza-Marañón Foreland Basin (PMFB), Peru, high annual rainfall and low seasonality overwhelm
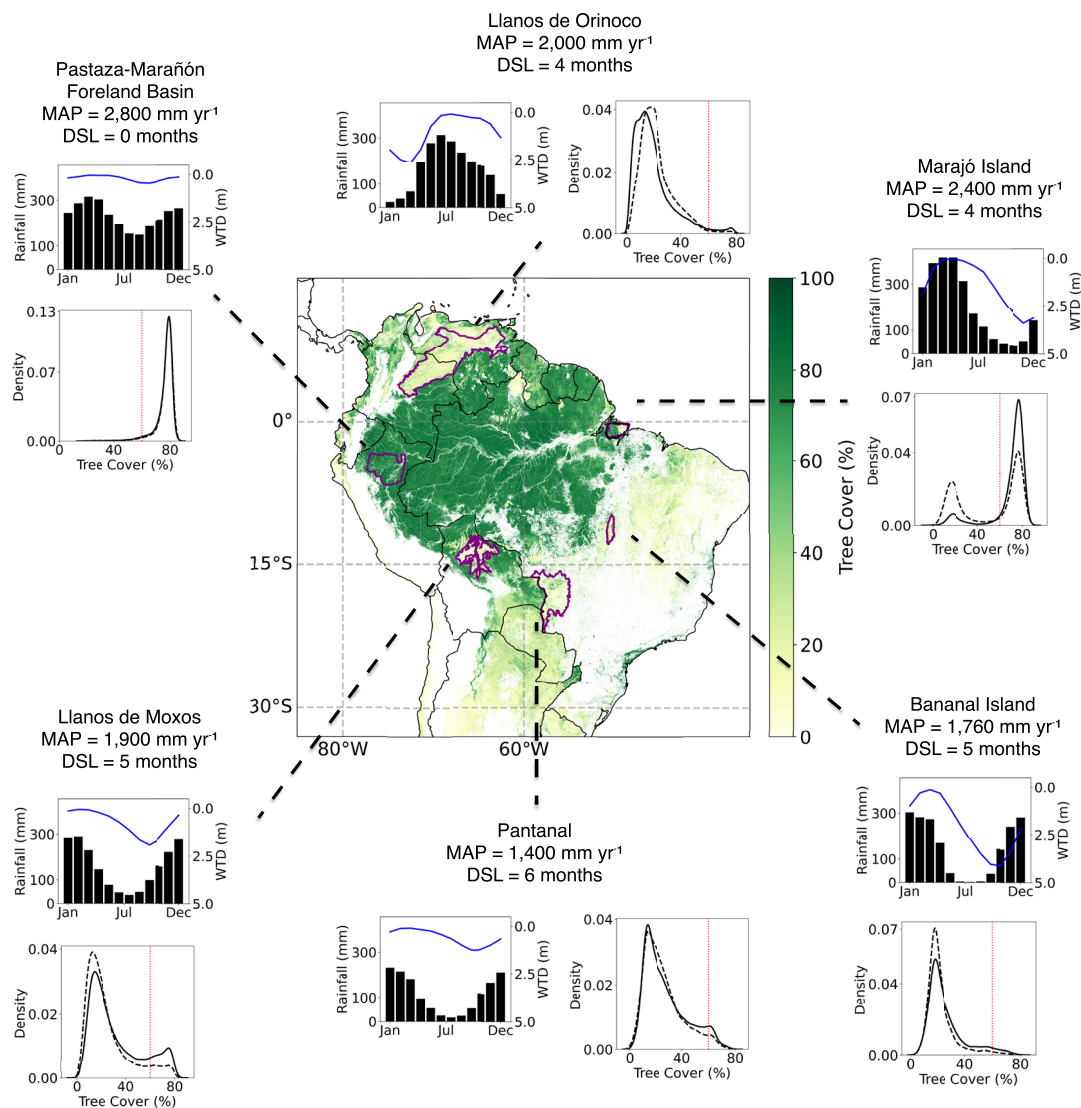
Fig. 3. Assessing the role of climate and drainage in shaping tree cover for six floodplains in tropical South America. The central map displays tree cover in tropical South America, with the selected floodplains highlighted. For each floodplain, we provide (1) MAP and dry season length (DSL) as measures of climatic stress; (2) mean monthly rainfall (black bars) and WT depth in waterlogged areas (blue line); and (3) tree cover distribution for double-stressed cells (dashed line) compared to non-double-stressed cells (solid line), measuring the hydrologic stress. The red dashed line shows the tree cover threshold between forest and savanna. Savanna prevalence increases with decreasing precipitation and increased seasonality (distributions shifting from *Right* to *Left*). Double-stress conditions favor savanna over forests under local climates, as indicated by the higher density of low tree cover in double-stressed areas. A detailed comparison of savanna and forest coverage in double-stressed and non-double-stressed areas for each floodplain can be found in *SI Appendix*, Table S5.

the possible negative influence of double stress by limiting WT variability and providing stable rainfall supply even when WT fluctuates, and both double-stressed and non-double-stressed areas have very similar tree cover distribution. As seasonality increases and rainfall reduces, the effects of double stress start to appear. In the Llanos de Orinoco, Venezuela, and Marajó Island, Brazil, the dry season extends for 4 mo, sufficient to generate a ~2.5 m drop in WT levels of waterlogged regions from wet to dry season. As such, savanna proportion increases in double-stressed areas (*SI Appendix*, Table S5). However, despite similar seasonality, higher annual rainfall in Marajó Island is associated with higher forest occurrence, with the same pattern observed for the Llanos de Moxos, Bolívia (higher rainfall, more forest) when compared to Bananal Island (more seasonal, less forest). At the extreme of the rainfall-seasonality gradient is the Brazilian Pantanal wetland, which shows very similar tree cover distribution for double-stressed and non-double-stressed areas, with only slightly less forests for double-stressed areas.

Future Changes in Double Stress

In the light of our findings, the pressing question of how present-day forests may shift to savannas under a warming climate may hinge on how the double-stressed landscape positions may shift in the future. We identify the landscape positions that may experience such shifts using a historic (1990 to 2000) and a future (2090 to 2100) hydrologic simulation for the Amazônia using the same model but forced by historic and future climate from the Hadley Center model (20). We focus our analyses on pixels which are presently classified as forest and not subject to double stress, but which, according to our future simulation, will be exposed to double stress and thus exposed to the risk of shifting into savannas.

Increased double stress from higher rainfall seasonality in the future simulation exposes large areas of tropical South America, particularly the interior of Amazônia, to the risk of vegetation shifts (Fig. 4). Floodplain forests of the Amazonas, Madeira, and

Upper Negro Rivers, recognized as some of the most diverse floodplain forests in the world, with a high level of endemism (21), are particularly affected in this simulation, together with forests on the toe slopes of the Andes and the Venezuelan forests which transition into the Llanos de Orinoco. Although we demonstrate that the hydrologic environment can potentially shift, vegetation shift is limited by biological processes. Fast vegetation response has been documented for burned igapó flooded forests in the Middle Rio Negro, with vegetation shifts toward "white-sand savannas" occurring on relatively short timescales (~40 y) (22). However, while the conditions for potential vegetation shift—the hydrological stress of alternating waterlogging and drought—may be present in a larger area in Central and Western Amazônia than previously thought, the magnitude and timing of vegetation change is likely to be controlled by local factors. Forest composition, function, and local environmental dynamics should play a key role in shaping the actual response of forest to the new double stress, and more research is needed to determine the vulnerability of each forest type to this framework of hydrological stress.

Discussion

The WT seasonality in lowlands is closely tied to rainfall seasonality. In the neotropics, the dry season can be absent in the Peruvian Amazônia to lasting 6 mo in southeastern Amazônia and the Brazilian Cerrado (23). During such long dry seasons, even waterlogged floodplains can experience temporary droughts, with WT falling far below the reach of the shallow roots, a characteristic feature of waterlogged ecosystems (6, 24). Fire also intensifies in the dry season, and due to the shallow exposed root mats of floodplain vegetation, fire can cause greater damage (25). Due to shorter favorable growth conditions and low nutrient levels (in black- and clearwater floodplains), tree recovery from fire is slow (22, 26). This opens a niche for sparser vegetation to occupy, especially fast growing C4 grasses, recognized as the earliest tropical floodplain occupants (3, 27). Increase in dryseason dead grass biomass fuels more fires, and associated feedback loops help prevent tree establishment on seasonally flooded and droughted landscape positions.

Such areas of alternating waterlogging and drought have been associated with hyperseasonal savannas (28) of dominantly herbaceous cover (29, 30), in part because roots of woody savanna species are waterlogging intolerant (18). Double-stressed savannas have a distinct floristic composition (29) from the more well-known Brazilian Cerrado vegetation, rich in eudicots (31). These hyperseasonal savannas are largely dominated by graminoids which couple aboveground phenological cycles with the waterlogging and drought cycles (29). Trees are largely excluded from community assemblages in these double-stressed areas, except for a few deciduous taxa that shed leaves in the dry season to avoid droughts. This strategy, however, requires higher nutrient availability (32), which is not the case in most neotropical savanna soils that are largely acidic and nutrient-poor (33). Graminoid species, on the other hand, can more easily cope with droughts. By coupling aerial biomass production with environmental cycles such as waterlogging and drought, these species are able to optimize productivity when conditions are less stressful (14, 29, 34). Ample field evidence shows that in the highly seasonal neotropics, while the elevated landscape positions support woody vegetation, the seasonally flooded and droughted lower slopes do not (35–39).

Our findings suggest that land hydrology may underlie forest–savanna coexistence under the same climatic conditions (Fig. 3), particularly in the rainfall bistability range (Fig. 1B and SI Appendix, Fig. S1) by creating conditions for double stress on trees. Nonetheless, land hydrology may also potentially contribute to the coexistence of both alternative stable states at the landscape level by regulating
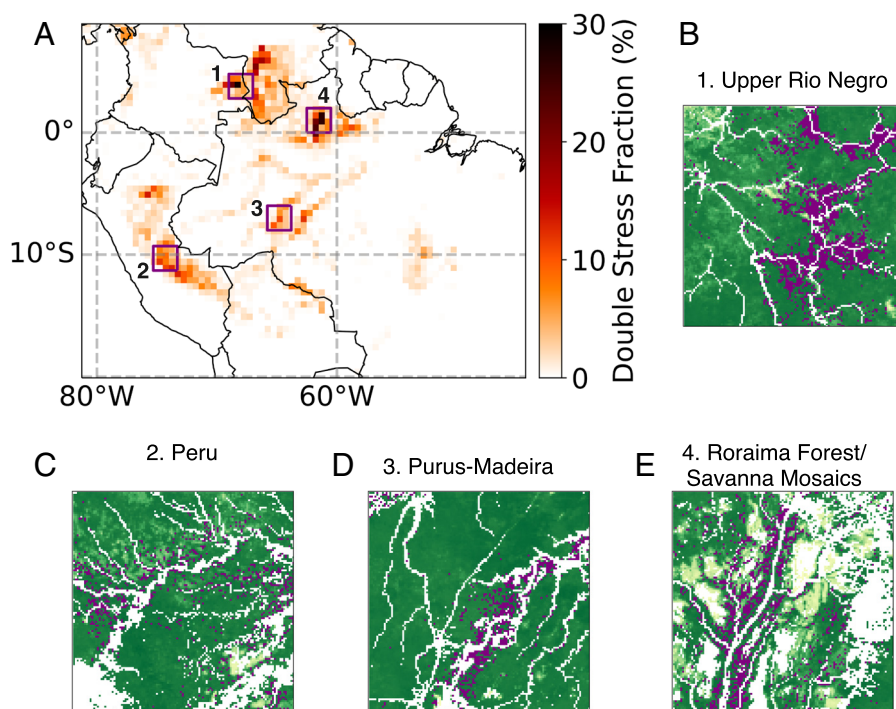

Fig. 4. Forest areas today that can be potentially converted to double-stressed, savanna-dominated conditions by the end of the 21st century. (A) Percent of a 0.25° window occupied by present forests exposed to future double stress, illustrating the effect of increased hydrological variability on the major floodplains and peatlands in tropical South America; (B–E) higher-resolution (2 km) Insets for 2° × 2° boxes in A showing tree cover (green-yellow, same as in Fig. 2) and forest pixels today that may change to savanna-like vegetation (in purple) at the end of the 21st century.

other types of stresses. For example, an exceptionally dry year could expose floodplain forests to more intense drought stress, favoring fires which could potentially force and trap vegetation into a more open-canopy, savanna-like state (26). Similarly, wetter than average years could extend waterlogging and reduce drought, favoring the establishment of drought- and fire-intolerant trees. It is therefore crucial to consider land hydrology as an environmental driver that operates at longer timescales than climate processes.

A comparison between present and future simulations of hydrologic stress shows that floodplain forests of the Amazonas, Madeira, and Upper Negro Rivers, recognized as some of the most diverse floodplain forests in the world, with a high level of endemism (21), will likely be affected. This differs from the prevalent understanding that forest loss from a warming climate will be mostly restricted to eastern and southern Amazônia (40–44), with some also pointing to higher risk for forests on the eastern slopes of the Andes (45). Accounting for double stress suggests that vegetation shifts can penetrate much deeper into the heart of Amazônia Forest, affecting 4,000,000 km^2 of forest (~1.4%) through tropical South America. Western Amazônia, home to some of the most biodiverse forests in the world (46, 47), might also be affected. Large areas of peatlands, such as the PMFB in Peru, might be exposed to reduced waterlogging and increased drought. These areas store large amounts of peat carbon, with the PMFB carbon stock estimated at 3.4 (0.44 to 8.15) PgC (48) and the entire lowland Peruvian Amazônia at 5.38 (2.55 to 10.58) PgC (49). Enhanced drainage, forest collapse, and increased fire frequency (26, 50) might thus affect large reservoirs of peat, preventing accumulation and leading to decomposition and consequent release of CO_2 into the atmosphere (51–53) accelerating warming. We argue that global change research can benefit from a sharpened focus on hydrologic change, which is driven by climate change but strongly mediated by the stable and structured terrain.

Materials and Methods

A detailed description of all methods is available in the accompanying *SI Appendix*. Below we summarize the methodology and data processing behind the main analyses described throughout the text.

Study Area and Data Processing. We focus on tropical South America, defined within the 35°S–15°N latitudinal range by previous studies on forest–savanna distribution across the continent (1, 54–56). To eliminate potential temperature influences on vegetation due to high altitude, which could mask the effects of water (our focus), we limit our analyses to regions below 1,200 m elevation, as in ref. 2, using the HydroSHEDS digital elevation model with a resolution of 1 km.

For tree cover data, we utilize the MODIS MOD44B v6 Vegetation Continuous Fields (VCF) product (57), at 250 m resolution for the year 2017. Pixels with tree cover of 60% or more are classified as forest, while those with less are designated as savanna (1, 54, 56). We exclude pixels affected by human-induced land-use changes that could artificially decrease tree cover. To do so, we use a combination of MAPBIOMAS Version 6 (58), MAPBIOMAS Amazonia Version 3, both at 3 m resolution, and the Copernicus Global Land Cover product at 100 m resolution. We use the MAPBIOMAS product where available, due to higher spatial resolution, and keep the Copernicus product elsewhere. We combine products according to the original resolution, applying a strict upscaling procedure to minimize human influence when upscaling is needed to match with other datasets (*SI Appendix*,

section 9). We upscale all data products to match the 1-km resolution of our hydrological model (see below and *SI Appendix*).

Land Hydrology Model and Hydrologic Stress. We use the output of a global hydrological model (5) which represents the land surface at a grid of 30-arcsecond cells, approximately 1 km each at the equator, allowing us to differentiate between different hydrological positions. The model is run on an hourly basis over a 15-y period from 2004 to 2018, enabling the resolution of event-to-seasonal dynamics. A more detailed description of the model as well as comparisons of river discharge, evapotranspiration, and WT depth is available in *SI Appendix*.

To quantify hydrologic stress, we follow the hydrologic niche theory of Silvertown et al. (1999) (8). We calculate the SEV to measure the frequency of waterlogging and drought stress at each landscape position. Drought stress SEV (*SI Appendix*, Fig. S12) is defined as the average number of months per year (over 15 y) where the WT falls below the 2 m threshold. Conversely, waterlogging SEV (*SI Appendix*, Fig. S13) is the number of months where the WT exceeds 0.25 m.

We also use a 2-km resolution hydrological model simulation of historical (end of the 20th century) and future (end of the 21st century) conditions (20). The model is forced with output from the Hadley Center Global Environment Model version 2 (HadGEM2-ES). Future simulation uses the Representative Concentration Pathways Scenario 8.5 (RCP8.5), which leads to ~940 ppm CO_2 by the end of the century and a 0.62-m mean sea level rise projected by the IPCC-AR5 (59). We use the same procedure of calculating SEVs to quantify the change in hydrological stress between historical and future conditions (Fig. 4).

Data, Materials, and Software Availability. Scripts necessary to reproduce the analyses pertaining to the main figures can be accessed at https://github.com/caiomattos/doublestress (60). HydroSHEDS Elevation data can be downloaded at https://www.hydrosheds.org/hydrosheds-core-downloads (61). MODIS MOD44B v6 VCF is available at https://lpdaac.usgs.gov/products/mod44bv006/ (62). MAPBIOMAS Brazil Version 6 is available at https://mapbiomas.org (63). MAPBIOMAS Amazonia Version 3 is available at https://amazonia.mapbiomas.org (64). Copernicus Global Land Cover is available at https://land.copernicus.eu/global/products/lc (65). ERA-5 Land atmospheric data are available at https://www.ecmwf.int/en/era5-land (17). All data necessary to reproduce the results of this manuscript are available at https://zenodo.org/record/7950934 (66). Previously published data were used for this work (https://doi.org/10.1038/s41586-021-03958-6) (5).

Author affiliations: ^aDepartment of Earth and Planetary Sciences, Rutgers University, New Brunswick, NJ 08854; ^bDepartment of Physics, Federal University of Santa Catarina, Florianópolis 88040-900, Brazil; ^cDepartment of Plant Biology, University of Campinas, Campinas 13083-862, Brazil; ^dGraduate Program in Ecology, Federal University of Santa Catarina, Florianópolis 88040-900, Brazil; ^eCRETUS, Non-Linear Physics Group, Faculty of Physics, Universidade de Santiago de Compostela, Santiago de Compostela 15782, Spain; and ^fDepartment of Civil and Environmental Engineering, Michigan State University, East Lansing, MI 48824

1. M. Hirota, M. Holmgren, E. H. V. Nes, M. Scheffer, Global resilience of tropical forest and savanna to critical transitions. *Science* **334**, 232–235 (2011).
2. A. C. Staver, S. Archibald, S. A. Levin, The global extent and determinants of savanna and forest as alternative biome states. *Science* **334**, 230–232 (2011).
3. I. Oliveras, Y. Malhi, Many shades of green: The dynamic tropical forest–savannah transition zones. *Philos. Trans. R. Soc. B* **371**, 20150308 (2016).
4. A. C. Staver, S. Archibald, S. Levin, Tree cover in sub-Saharan Africa: Rainfall and fire constrain forest and savanna as alternative stable states. *Ecology* **92**, 1063–1072 (2011).
5. G. Miguez-Macho, Y. Fan, Spatiotemporal origin of soil water taken up by vegetation. *Nature* **598**, 624–628 (2021).
6. Y. Fan, G. Miguez-Macho, E. G. Jobbágy, R. B. Jackson, C. Otero-Casal, Hydrologic regulation of plant rooting depth. *Proc. Natl. Acad. Sci. U.S.A.* **114**, 10572–10577 (2017).

7. P. Parolin, Morphological and physiological adjustments to waterlogging and drought in seedlings of Amazonian floodplain trees. *Oecologia* **128**, 326–335 (2001).
8. J. Silvertown, M. E. Dodd, D. J. G. Gowing, J. O. Mountford, Hydrologically defined niches reveal a basis for species richness in plant communities. *Nature* **400**, 61–63 (1999).
9. Y. N. Araya *et al.*, A fundamental, eco-hydrological basis for niche segregation in plant communities. *New Phytol.* **189**, 253–258 (2011).
10. G. García-Baquero, J. Silvertown, D. J. Gowing, C. J. Valle, Dissecting the hydrological niche: Soil moisture, space and lifespan. *J. Veg. Sci.* **27**, 219–226 (2016).
11. Ü. Niinemets, F. Valladares, Tolerance to shade, drought, and waterlogging of temperate northern hemisphere trees and shrubs. *Ecol. Monogr.* **76**, 521–547 (2006).
12. P. J. Grubb, Trade-offs in interspecific comparisons in plant ecology and how plants overcome proposed constraints. *Plant Ecol. Divers.* **9**, 3–33 (2016).
13. C. Bakker, P. M. van Bodegom, H. J. M. Nelissen, R. Aerts, W. H. O. Ernst, Preference of wet dune species for waterlogged conditions can be explained by adaptations and specific recruitment requirements. *Aquat. Bot.* **86**, 37–45 (2007).
14. M. T. F. Piedade, W. J. Junk, S. P. Long, The productivity of the C_4 Grass *Echinochloa Polystachya* on the Amazon floodplain. *Ecology* **72**, 1456–1463 (1991).
15. M. Rueda, O. Godoy, B. A. Hawkins, Trait syndromes among North American trees are evolutionarily conserved and show adaptive value over broad geographic scales. *Ecography* **41**, 540–550 (2018).
16. Y. Fan, H. Li, G. Miguez-Macho, Global patterns of groundwater table depth. *Science* **339**, 940–943 (2013).
17. Y. Muñoz Sabater, Data from "ERA5-Land monthly averaged data from 1950 to 1980." *Copernic. Clim. Change Serv. C3S Clim.* Data Store CDS. https://www.ecmwf.int/en/era5-land. Accessed 5 April 2022.
18. A. T. D. Oliveira-Filho, G. J. Shepherd, F. R. Martins, W. H. Stubblebine, Environmental factors affecting physiognomic and floristic variation in an area of cerrado in central Brazil. *J. Trop. Ecol.* **5**, 413–431 (1989).
19. P. Parolin, F. Wittmann, Struggle in the flood: Tree responses to flooding stress in four tropical floodplain systems. *AoB Plants* **2010**, plq003 (2010).
20. Y. N. Pokhrel, Y. Fan, G. Miguez-Macho, Potential hydrologic changes in the Amazon by the end of the 21st century and the groundwater buffer. *Environ. Res. Lett.* **9**, 084004 (2014).
21. F. Wittmann *et al.*, Tree species composition and diversity gradients in white-water forests across the Amazon Basin. *J. Biogeogr.* **33**, 1334–1347 (2006).
22. B. M. Flores, M. Holmgren, White-sand savannas expand at the core of the Amazon after forest wildfires. *Ecosystems* **24**, 1624–1637 (2021).
23. J. A. Marengo, B. Liebmann, V. E. Kousky, N. P. Filizola, I. C. Wainer, Onset and end of the rainy season in the Brazilian Amazon Basin. *J. Clim.* **14**, 833–852 (2001).
24. F. R. C. Costa, J. Schietti, S. C. Stark, M. N. Smith, The other side of tropical forest drought: Do shallow water table regions of Amazonia act as large-scale hydrological refugia from drought? *New Phytol.* **237**, 714–733 (2022).
25. R. C. Rivaben *et al.*, Do fire and flood interact to determine forest islet structure and diversity in a Neotropical wetland? *Flora* **281**, 151874 (2021).
26. B. M. Flores *et al.*, Floodplains as an Achilles' heel of Amazonian forest resilience. *Proc. Natl. Acad. Sci. U.S.A.* **114**, 4442–4446 (2017).
27. F. Mouillot, C. B. Field, Fire history and the global carbon budget: A 1° x 1° fire history reconstruction for the 20th century. *Glob. Change Biol.* **11**, 398–420 (2005).
28. G. Sarmiento, "The Savannas of tropical America" in *En: Tropical savannas*, F. Bourliere, Ed. (Elsevier, Amsterdam, NL, 1983), pp. 245–288.
29. G. Sarmiento, M. Pinillos, M. P. da Silva, D. Acevedo, Effects of soil water regime and grazing on vegetation diversity and production in a hyperseasonal savanna in the Apure Llanos, Venezuela. *J. Trop. Ecol.* **20**, 209–220 (2004).
30. M. V. Cianciaruso, M. Antônio Batalha, I. Aurélio da Silva, Seasonal variation of a hyperseasonal cerrado in Emas National Park, central Brazil. *Flora Morphol. Distrib. Funct. Ecol. Plants* **200**, 345–353 (2005).
31. M. G. de Moraes, M. A. M. de Carvalho, A. C. Franco, C. J. Pollock, R. de C. L. Figueiredo-Ribeiro, Fire and drought: Soluble carbohydrate storage and survival mechanisms in Herbaceous plants from the Cerrado. *BioScience* **66**, 107–117 (2016).
32. R. S. Oliveira *et al.*, Linking plant hydraulics and the fast–slow continuum to understand resilience to drought in tropical ecosystems. *New Phytol.* **230**, 904–923 (2021).
33. M. Bustamante *et al.*, Potential impacts of climate change on biogeochemical functioning of Cerrado ecosystems. *Braz. J. Biol.* **72**, 655–671 (2012).
34. G. Sarmiento, Adaptive strategies of perennial grasses in South American savannas. *J. Veg. Sci.* **3**, 325–336 (1992).
35. P. A. Furley, "Edaphic changes at the forest-savanna boundary with particular reference to the neotropics" in *Nature and Dynamics of Forest-Savanna Boundaries*, P. A. Furley, J.Proctor, J. A. Ratter, Eds. (CRC Press, London, 1992).
36. J. A. Ratter, "Transitions between cerrado and forest vegetation in Brazil" in *Nature and Dynamics of Forest-Savanna Boundaries* (Chapman Hall, New York, 1992).
37. J. Thompson, J. Proctor, V. Viana, J. A. Ratter, D. A. Scott, "The forest-savanna boundary on Maracá Island, Roraima, Brazil: An investigation of two contrasting transects" in *Nature and Dynamics of Forest-Savanna Boundaries*. (Chapman & Hall, Reino Unido, London, 1992).
38. D. R. Rossatto, L. d. Carvalho Ramos Silva, R. Villalobos-Vega, L. d. S. L. Sternberg, A. C. Franco, Depth of water uptake in woody plants relates to groundwater level and vegetation structure along a topographic gradient in a neotropical savanna. *Environ. Exp. Bot.* **77**, 259–266 (2012).
39. R. de O. Xavier, M. B. Leite, K. Dexter, D. M. da Silva Matos, Differential effects of soil waterlogging on herbaceous and woody plant communities in a Neotropical savanna. *Oecologia* **190**, 471–483 (2019).
40. M. D. Oyama, C. A. Nobre, A new climate-vegetation equilibrium state for Tropical South America: A new climate-vegetation state. *Geophys. Res. Lett.* **30**, 2199 (2003).
41. D. C. Nepstad, C. M. Stickler, B. S. - Filho, F. Merry, Interactions among Amazon land use, forests and climate: Prospects for a near-term forest tipping point. *Philos. Trans. R. Soc. Lond. B Biol. Sci.* **363**, 1737–1746 (2008).
42. Y. Malhi *et al.*, Exploring the likelihood and mechanism of a climate-change-induced dieback of the Amazon rainforest. *Proc. Natl. Acad. Sci. U.S.A.* **106**, 20610–20615 (2009).
43. M. T. Coe *et al.*, Deforestation and climate feedbacks threaten the ecological integrity of south–southeastern Amazonia. *Philos. Trans. R. Soc. Lond. B Biol. Sci.* **368**, 20120155 (2013).
44. J. V. Tavares *et al.*, Basin-wide variation in tree hydraulic safety margins predicts the carbon balance of Amazon forests. *Nature* **617**, 111–117 (2023).
45. D. C. Zemp *et al.*, Self-amplified Amazon forest loss due to vegetation-atmosphere feedbacks. *Nat. Commun.* **8**, 14681 (2017).
46. H. Ter Steege *et al.*, A spatial model of tree α-diversity and tree density for the Amazon. *Biodivers. Conserv.* **12**, 2255–2277 (2003).
47. F. M. Sabatini *et al.*, Global patterns of vascular plant alpha diversity. *Nat. Commun.* **13**, 4683 (2022).
48. F. C. Draper *et al.*, The distribution and amount of carbon in the largest peatland complex in Amazonia. *Environ. Res. Lett.* **9**, 124017 (2014).
49. A. Hastie *et al.*, Risks to carbon storage from land-use change revealed by peat thickness maps of Peru. *Nat. Geosci.* **15**, 369–374 (2022).
50. A. A. Alencar, P. M. Brando, G. P. Asner, F. E. Putz, Landscape fragmentation, severe drought, and the new Amazon forest fire regime. *Ecol. Appl.* **25**, 1493–1505 (2015).
51. S. E. Page *et al.*, The amount of carbon released from peat and forest fires in Indonesia during 1997. *Nature* **420**, 61–65 (2002).
52. A. Hooijer *et al.*, Current and future CO2 emissions from drained peatlands in Southeast Asia. *Biogeosciences* **7**, 1505–1514 (2010).
53. J. van Lent, K. Hergoualc'h, L. Verchot, O. Oenema, J. W. van Groenigen, Greenhouse gas emissions along a peat swamp forest degradation gradient in the Peruvian Amazon: Soil moisture and palm roots effects. *Mitig. Adapt. Strateg. Glob. Change* **24**, 625–643 (2019).
54. M. Holmgren, M. Hirota, E. H. van Nes, M. Scheffer, Effects of interannual climate variability on tropical tree cover. *Nat. Clim. Change* **3**, 755–758 (2013).
55. A. Staal, S. C. Dekker, C. Xu, E. H. van Nes, Bistability, spatial interaction, and the distribution of tropical forests and savannas. *Ecosystems* **19**, 1080–1091 (2016).
56. E. H. van Nes, M. Hirota, M. Holmgren, M. Scheffer, Tipping points in tropical tree cover: Linking theory to data. *Glob. Change Biol.* **20**, 1016–1021 (2014).
57. C. DiMiceli *et al.*, MOD44B MODIS/Terra vegetation continuous fields yearly L3 global 250m SIN grid V006. (2015). https://doi.org/10.5067/MODIS/MOD44B.006. 12 November 2021.
58. C. M. Souza *et al.*, Reconstructing three decades of land use and land cover changes in Brazilian biomes with landsat archive and earth engine. *Remote Sens.* **12**, 2735 (2020).
59. Intergovernmental Panel on Climate Change, Ed., "Sea level change" in *Climate Change 2013–The Physical Science Basis* (Cambridge University Press, ed. 1, 2014), pp. 1137–1216.
60. C. R. C. Mattos, Analysis and plotting scripts. GitHub. https://github.com/caiomattos/doublestress. Deposited 15 May 2023.
61. B. Lehner, K. Verdin, A. Jarvis, New global hydrography derived from spaceborne elevation data. *Eos, Transactions, American Geophysical Union*, **89**, 93–94, https://doi.org/10.1029/2008eo100001 (2008).
62. C. Dimiceli, M. Carroll, R. Sohlberg, D. H. Kim, M. Kelly, MOD44B MODIS/terra vegetation continuous fields yearly L3 global 250m SIN grid V006. NASA EOSDIS Land Processes DAAC. 10.5067/MODIS/MOD44B.006. Accessed 20 March 2022.
63. C. M. Souza *et al.*, Reconstructing Three Decades of Land Use and Land Cover Changes in Brazilian Biomes with Landsat Archive and Earth Engine. *Remote Sens*, **12**, 10.3390/rs12172735 (2020).
64. MapBiomas Amazonia Project, Collection Version 3 of Amazonian Annual Land Cover & Land Use Map Series. https://amazonia.mapbiomas.org. Accessed 20 March 2022.
65. M. Buchhorn *et al.*, Copernicus Global Land Service: Land Cover 100m, collection 3, epoch 2017, Globe 2020, 10.5281/zenodo.3518036. Accessed 20 March 2022.
66. C. R. C. Mattos *et al.*, Data for "Double stress of waterlogging and drought drives forest–savanna coexistence." Zenodo. https://zenodo.org/record/7950934. Deposited 20 May 2023.